Light-Scattering and Phase-Separation Studies on Cyclohexane Solutions of Four-Arm Star Polystyrene

Ken Terao, Mitsuhiro Okumoto, Yo Nakamura,*,† Takashi Norisuye, and Akio Teramoto‡

Department of Macromolecular Science, Osaka University, Machikaneyama-cho 1-1, Toyonaka, Osaka 560-0043, Japan

Received May 27, 1998; Revised Manuscript Received July 14, 1998

ABSTRACT: Light-scattering and phase-separation experiments were performed on cyclohexane solutions of four narrow-distribution samples of four-arm star polystyrene with molecular weights of 8.5×10^4 to 1.4×10^6, and the results were compared with literature data for linear polystyrene in cyclohexane. The upper critical solution temperatures T_c for the star polymer were systematically lower than those for the linear polymer, showing a considerable effect of chain branching on phase separation. The apparent second virial coefficients J of light scattering for the two polymers, plotted against $\phi/P^{0.1}$ at a fixed temperature below Θ, happened to form a composite curve at high polymer concentrations, regardless of the relative degree of polymerization P (ϕ denotes the polymer volume fraction), whereas they appreciably differed at low concentrations, reflecting the finding that the (true) second virial coefficient for the star polymer is significantly larger than that for the linear polymer below Θ. The chemical potentials of the solvent and solute components derived from the J data were shown to explain the phase diagrams of the two systems fairly well. Thus it was concluded that the difference in T_c between four-arm star and linear polystyrenes arises primarily from the difference in J in dilute solution.

Introduction

Prediction of phase relationships of polymer solutions has long been the subject of polymer thermodynamics,[1,2] but some fundamental problems are still left almost unexplored. An example is the effect of chain branching on the phase diagram. Cowie et al.[3] found from cloud point measurements on cyclohexane solutions of star polystyrenes that when compared at the same molecular weight, upper critical solution temperatures for them are systematically lower than those for linear polystyrene. Similar findings were also reported for random- and star-branched polystyrenes in cyclohexane by Sato et al.[4] and Yokoyama et al.,[5] respectively. It is natural to discuss such differences in phase behavior in terms of the chemical potentials of the solvent and solute components, which may be determined either experimentally or theoretically. For an experimental approach, light-scattering measurements in the dilute through semidilute regimes may be appropriate, because they give the differential chemical potential of the solvent with high precision.[6−9] Although osmotic-pressure[10] and light-scattering[11] data are available for semidilute solutions of star polymers in good solvents, no such data for poor solvent systems are as yet reported.

In this work, we made light-scattering measurements on cyclohexane solutions of four-arm star polystyrene samples with weight-average molecular weights M_w of 8.5×10^4 to 1.4×10^6 and determined the chemical potential of the solvent as a function of temperature T, polymer concentration, and M_w, following essentially the same approach as that taken by Einaga et al.[9] for linear polystyrene in cyclohexane. Phase equilibrium experiments on the star polymer + solvent system were also carried out to see the difference in phase separation behavior between the star and linear polystyrenes and to analyze the data in terms of the chemical potentials.

Experimental Section

Polymer Samples. Four-arm star polystyrene samples 4S22, 4S39, 4S77′, and 4S384 were chosen from those used in previous studies.[12,13] These samples had been prepared by anionic polymerization and well-fractionated; they are sufficiently narrow in molecular weight distribution and have exactly four arms.

Light Scattering. Scattered intensities were measured on a Fica-50 light-scattering photometer in an angular range from 30 to 150° using vertically polarized light of 436 and 546 nm wavelengths. Benzene at 25 °C was used as the reference liquid, whose Rayleigh ratio was taken to be 46.5×10^{-6} cm^{-1} for 436 nm and 16.1×10^{-6} cm^{-1} for 546 nm.[14] Its depolarization ratio was determined to be 0.41 and 0.40 for 436 and 546 nm, respectively, by the method of Rubingh and Yu.[15] Polymer solutions were optically clarified by filtration through a Teflon membrane.

Values of the specific refractive index increment $\partial n/\partial c$ for four-arm star polystyrene in cyclohexane at 546 nm were evaluated from the relation

$$\partial n/\partial c = 0.1535 + 4.5 \times 10^{-4}(T/°\mathrm{C}) + 87M_w^{-1} \qquad (\mathrm{cm^3\ g^{-1}})$$

determined in this work and those at 436 nm from the previously determined relation.[13]

Correction of Scattering Intensities. (1) Absorbance. Absorbances A of cyclohexane solutions of 4S39, 4S384, and one linear low-molecular weight polystyrene sample (M_w = 3300) were measured on a double-beam ultraviolet spectrometer (Shimadzu UV-200) using a quartz cell of 1 cm thickness. Measurements were also made on benzene solutions of 4S22, 4S39, 4S384, and some linear polystyrene samples (Toso's standard samples) of different molecular weights.

Figure 1 shows the concentration dependence of A for 4S39 in cyclohexane at 436 nm and the indicated temperatures, where c represents the polymer mass concentration. Maxima

† Current address: The University of Alabama at Birmingham, Birmingham, AL 35294.

‡ Current address: Research Organization of Science and Engineering, Ritsumeikan University, Noji-higashi, Kusatsu, Shiga 525-8577, Japan.

S0024-9297(98)00839-0 CCC: $15.00
Published on Web 09/10/1998

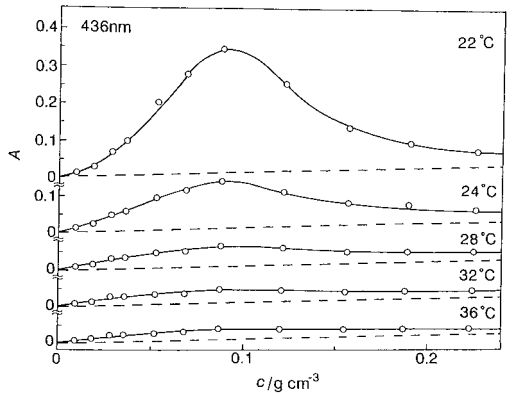

Figure 1. Concentration dependence of absorbance A for cyclohexane solutions of four-arm star polystyrene sample 4S39 at the indicated temperatures and wavelength of light.

due to critical opalescence can be seen at $c \sim 0.09$ g cm^{-3}. Such pronounced attenuation of light suggested substantial effects of absorption, turbidity, and multiple scattering on the reduced excess scattering intensity R_θ at scattering angle θ. In fact, plots of K/R_0 vs k^2 for the incident beams of 436 and 546 nm did not accord with each other near the critical point, and they bent considerably upward at both low and high angles. Here, K is the optical constant and k the magnitude of the scattering vector.

The dashed line at each T in Figure 1 represents the contribution from the absorption of light by the polymer, estimated from the absorption coefficient γ for four-arm star polystyrene in benzene; this estimation is based on our finding that the difference in γ between cyclohexane and benzene solutions of linear low-molecular weight polystyrene and that between linear and four-arm star polystyrene in benzene were negligibly small. The values of γ in benzene, which were 0.16 and 0.08 cm^2 g^{-1} for 436 and 546 nm (for $M_w > 4 \times 10^4$ and at any T studied), respectively, are used for the ensuing analysis of scattering intensity data for four-arm star polystyrene in cyclohexane. We note that the turbidity τ at a given c is proportional to the difference between the solid and dashed curves and is given by 2.303 (A/l_1 - γc), with l_1 being the path length of light in the cell.

(2) Determination of R_θ. If, as is the case for our star samples in cyclohexane near the Θ point, the radius of gyration is not very large,[13] R_θ may be represented by a linear function of $\sin^2(\theta/2)$ in a good approximation. In this case, it can be shown that R_{90}, i.e., R_θ at $\theta = 90°$, is related to τ by

$$R_{90} = 3\tau/8\pi \tag{1}$$

In actuality, however, the apparent (or measured) scattering intensity $R_{90,app}$ at 90°, corrected for absorption and turbidity by a factor exp(2.303A), was a quadratic function of τ. This indicates that the effect of multiple scattering is significant for our system and that the apparent scattering intensity $R_{\theta,app}$ at θ should have a form

$$R_{\theta,app} \exp(2.303\gamma lc + \tau l) = R_\theta + f(\theta)\tau^2 \tag{2}$$

where l is the path length in the light scattering cell (=2.2 cm). The function $f(\theta)$ associated with the multiple scattering was determined as $f(\theta) = 0.07 + 0.09 \sin\theta$ by empirical fitting of $R_{\theta,app} \exp(2.303\gamma lc + \tau l)$ on the assumption that R_θ is a linear function of $\sin^2(\theta/2)$ and $f(\theta)$ is symmetrical about $\theta = 90°$.

In the determination of the desired R_θ from the measured $R_{\theta,app}$, τ was first evaluated for each solution by solving eq 2 with $\theta = 90°$ and eq 1, since absorption data were taken only for some of the solutions studied by light scattering. Then, with τ so obtained, R_θ was calculated as a function of θ using eq 2.

Phase Separation Experiment. Phase separation experiments were carried out using a Brice-type cell (2 cm square bottom and 5 cm height) composed of two triangular sections, one filled with a test solution and the other with the pure solvent.[16] The cell stoppered with a Teflon cap was fixed in the inner bath of a double water thermostat, and the temperature of the inner bath was controlled within ±0.01 °C. The initial polymer concentration of the test solution was adjusted near the critical concentration.

Red laser beams were incident to the upper and lower parts of the cell, and the polymer concentrations in the phase-separated solutions were determined by differential refractometry with a photodiode as the detector fixed on a traveling arm at the distance 65 cm from the cell. The instrument was calibrated with four-arm star polystyrene solutions (samples 4S22 and 4S39) of known concentrations at 20, 25, and 30 °C. No substantial difference was found between the calibration constants for the two samples. The constants at the other temperatures were obtained by interpolation or extrapolation. The polymer volume fraction thus determined was accurate to ±0.0015.

Equilibrium was attained 6 h to 2 days after phase separation. This was ensured by monitoring the change in polymer concentration with time.

Results

Apparent Second Virial Coefficient. The zero-angle value of R_θ, R_0, is related to the chemical potential μ_0 of the solvent by[6,7]

$$\frac{K'\phi}{R_0} = -\frac{1}{RT}\frac{\partial\mu_0}{\partial\phi} \tag{3}$$

Here, ϕ is the volume fraction of the polymer, R the gas constant, T the absolute temperature, and K' the constant defined by

$$K' = \frac{4\pi^2 n^2}{N_A \lambda_0^4} V_0 \left(\frac{\partial n}{\partial\phi}\right)^2 \tag{4}$$

wherein N_A is the Avogadro constant, n the refractive index of the solution, λ_0 the wavelength of the incident light, and V_0 the molar volume of the solvent. If the apparent second virial coefficient $J(\phi)$ of light scattering is introduced by[9]

$$\frac{K'\phi}{R_0} = \frac{1}{P} + 2\phi J(\phi) \tag{5}$$

μ_0 is expressed as

$$\frac{\mu_0 - \mu_0^\circ}{RT} = -\frac{\phi}{P} - 2\int_0^\phi u J(u)\, du \tag{6}$$

Here, $\mu_0°$ is the chemical potential of the solvent in the pure state and P is the relative degree of polymerization defined by $M_w v_p/V_0$ with the specific volume v_p of the polymer.

Figure 2 illustrates the plots of J [≡$J(\phi)$] vs ϕ for sample 4S39 at temperatures between 22 and 36 °C. Here, ϕ has been calculated from the polymer weight fraction w using the relation $\phi = v_p w/[v_p w + v_0(1 - w)]$ with v_0 (the specific volume of cyclohexane) = 1.2924 cm^3 g^{-1} and $v_p = 0.9337$ cm^3 g^{-1} (both at 25 °C);[13] to be consistent with the above definition of P, v_0 and v_p have been regarded as temperature-independent. It can be seen that the infinite-dilution values of J (denoted below as J_0) are larger at higher T. This is the direct reflection of the T-dependence of the second virial coefficient A_2

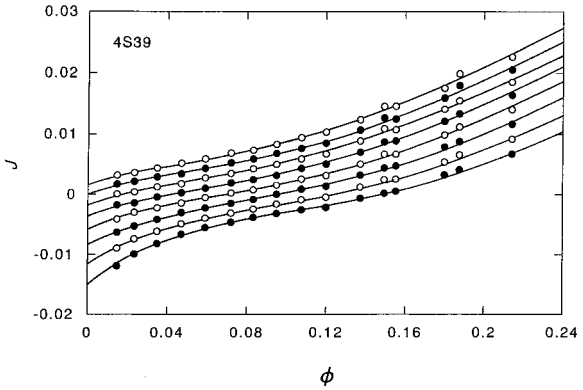

Figure 2. Plots of J vs ϕ for sample 4S39 in cyclohexane. The temperatures are 36, 34, 32, 30, 28, 26, 24, and 22 °C from top to bottom. Lines are eye guides.

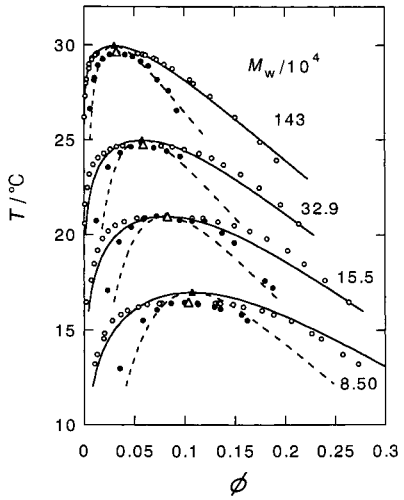

Figure 3. Phase diagrams for cyclohexane solutions of four-arm star polystyrene samples with indicated M_w: unfilled circles, coexisting-phase concentrations; filled circles, spinodals; unfilled triangles, experimental critical points; solid line, calculated binodal; dashed line, calculated spinodal; filled triangles, calculated critical points (see text).

which is related to J_0 by

$$A_2 = \frac{v_p^2}{V_0} J_0 \tag{7}$$

The initial slope of the J vs ϕ curve at $\phi = 0$ is proportional to the third virial coefficient, which is known to be positive at the Θ temperature and become larger as the temperature increases or decreases from Θ.[13] The slope of the curve first decreases with increasing ϕ and then increases after passing through an inflection point. For the convenience of our presentation, the ϕ regions below and above the inflection point are referred to as the *dilute* and *concentrated* ones, respectively. The former region becomes narrower with increasing temperature. All the observed features of J are similar to those found for linear polystyrene in cyclohexane by Einaga et al.[9]

Coexisting Curves. The unfilled circles in Figure 3 show the coexisting phase concentrations determined from our phase separation experiment. With decreasing molecular weight, the phase separation temperature becomes lower and the width of the two-phase region becomes wider. These features are similar to what is known for linear polymers.[1,2] The present phase separation data together with the previously determined molecular weights[13] are presented in Table 1, in which ϕ' and ϕ'' denote ϕ for the coexisting dilute and concentrated phases, respectively.

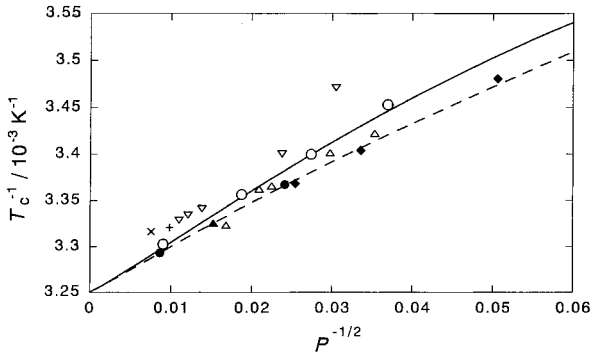

Figure 4. Plots of T_c^{-1} vs $P^{-1/2}$ for star [○, $f = 4$ (present data); △, $f = 3$ (ref 3); ▽, $f = 6-9$ (ref 3); +, $f = 6.3$ (ref 5); ×, $f = 11.1$ (ref 5)] and linear (●, ref 16; ◆, ref 17; ▲, ref 18) polystyrenes in cyclohexane. Solid line, calculated values for $f = 4$; dashed line, calculated values for $f = 2$ (linear) (see text).

The critical temperature T_c and the critical concentration ϕ_c for each sample were determined with the aid of the known critical exponents for linear polystyrene, i.e., by extrapolation[5] of T vs the $(\phi'' - \phi')^{1/0.327}$ plot to $\phi'' - \phi' = 0$ and the $(\phi' + \phi'')/2$ vs the $T_c - T$ plot to $T_c - T = 0$, respectively. The unfilled triangles in Figure 3 represent the critical points thus determined. The numerical results for the critical points are summarized in Table 2.

The values of T_c^{-1} are plotted against $P^{-1/2}$ in Figure 4, along with literature data for cyclohexane solutions of linear[16-18] and star polystyrenes with the arm number $f = 3$,[3] 6−9,[3] and 6.3 and 11.1 (on average).[5] It can be seen that T_c^{-1} is higher for a larger f at finite P but converges to a common ordinate intercept corresponding to $\Theta = 34.5$ °C at least for $f \leq 4$. The solid and dashed lines are explained in the Discussion.

Spinodals. Our K'/R_0 data, plotted against T^{-1} for each solution, were extrapolated to $K'/R_0 = 0$ to determine the spinodal temperature.[7] The filled circles in Figure 3 represent the spinodal points so obtained. As expected, each spinodal appears inside the corresponding binodal and touches the latter tangentially at the critical point. The numerical results for the spinodal points are summarized in Table 3.

Discussion

Empirical Equation for *J*. It is known that the concentration dependence of the reduced osmotic pressure for semidilute solutions of flexible polymer + good solvent systems is represented approximately by a function[10,19] only of c/c^* or ϕ/ϕ^* (c^* and ϕ^* denote the overlap mass concentration and volume fraction of polymer, respectively). This implies that plots of J vs $P^{1/2}\phi$ for different P form a composite curve, since ϕ^* is proportional to $P^{-1/2}$. For the linear or star polystyrene + cyclohexane system, however, such a relation does not hold.

After some trials, we found that when plotted against $\bar{\phi}$ ($\equiv \phi/P^{0.1}$), our J data for different molecular weights in the *concentrated region* form a composite curve at any fixed temperature below Θ. This is shown in Figure 5 with various unfilled symbols, where data (filled symbols) for linear polystyrene samples[8,9] are included. Interestingly, all the plotted points except in the *dilute*

Table 1. Concentrations of Four-Arm Star Polystyrene in Separated Phases of Cyclohexane Solutions

4S22 ($M_w = 8.50 \times 10^4$)			4S39 ($M_w = 1.55 \times 10^5$)			4S77′ ($M_w = 3.29 \times 10^5$)			4S384 ($M_w = 1.43 \times 10^6$)		
T/°C	ϕ'	ϕ''	T/°C	ϕ'	ϕ''	T/°C	ϕ'	ϕ''	T/°C	ϕ'	ϕ''
16.4_1	0.0774	0.1307	20.9_1	0.0603	0.1077	24.7_0	0.0386	0.0769	29.5_8	0.0134	0.0532
16.4_0	0.0752	0.1340	20.8_9	0.0528	0.1183	24.6_4	0.0323	0.0879	29.5_7	0.0133	0.0540
16.4_0	0.0746	0.1354	20.7_0	0.0399	0.1332	24.5_1	0.0260	0.1001	29.5_3	0.0121	0.0585
16.3_5	0.0627	0.1483	20.5_0	0.0310	0.1494	24.3_0	0.0198	0.1146	29.5_2	0.0118	0.0588
16.2_2	0.0540	0.1584	20.2_0	0.0240	0.1647	24.0_7	0.0138	0.1268	29.4_8	0.0113	0.0612
16.0_3	0.0432	0.1769	19.8_0	0.0184	0.1817	23.7_1	0.0089	0.1389	29.3_2	0.0080	0.0697
15.8_2	0.0365	0.1884	19.1_8	0.0134	0.2024	23.2_1	0.0051	0.1558	29.2_5	0.0080	0.0720
15.5_0	0.0283	0.2063	18.4_8	0.0101	0.2190	22.5_0	0.0033	0.1745	29.0_0	0.0050	0.0799
14.8_3	0.0204	0.2266	17.6_1	0.0072	0.2398	21.6_2	0.0008	0.1954	28.7_8	0.0050	0.0879
14.5_5	0.0196	0.2360	16.4_6	0.0022	0.2637	20.6_0	0.0006	0.2137	28.2_0	0.0025	0.1053
13.7_1	0.0129	0.2573							27.9_9	0.0018	0.1090
13.2_0	0.0107	0.2730							27.3_0	0.0010	0.1257
									26.2_0	0.0001	0.1502
									24.9_0		0.1753
									23.9_5		0.1916

Table 2. Critical Points for Cyclohexane Solutions of Four-Arm Star Polystyrene

sample	T_c/°C	ϕ_c
4S22	16.4_5	0.1040
4S39	20.9_8	0.0832
4S77′	24.7_7	0.0590
4S384	29.6_5	0.0325

Table 3. Spinodals for Cyclohexane Solutions of Four-Arm Star Polystyrene

4S22		4S39		4S77′		4S384	
ϕ	T/°C	ϕ	T/°C	ϕ	T/°C	ϕ	T/°C
0.035 77	12.9_7	0.023 41	17.0_8	0.012 23	20.7_5	0.006 05	26.6_5
0.058 37	15.5_3	0.034 75	19.6_3	0.023 68	23.5_9	0.009 90	28.1_5
0.072 52	16.0_8	0.046 94	20.4_1	0.036 17	24.3_4	0.010 16	28.2_8
0.086 56	16.4_1	0.058 92	20.8_4	0.046 69	24.6_5	0.013 68	28.9_6
0.100 1	16.4_5	0.071 85	21.0_1	0.057 30	24.8_7	0.018 84	29.2_8
0.112 6	16.4_1	0.083 19	20.9_2	0.069 32	24.6_0	0.025 50	29.5_1
0.113 3	16.3_7	0.094 95	20.7_9	0.082 51	24.4_2	0.033 41	29.6_1
0.129 6	16.2_4	0.107 5	20.7_5	0.095 51	24.1_6	0.040 81	29.5_1
0.135 4	16.1_2	0.120 0	20.7_5			0.048 60	29.4_2
0.156 4	15.8_3	0.137 2	20.1_1			0.056 49	29.1_5
0.162 1	15.5_3	0.149 4	19.5_9			0.064 12	28.9_2
		0.179 9	17.5_9			0.072 65	28.1_9
		0.187 5	17.2_1			0.084 18	27.6_0
						0.092 14	26.5_7

region fall almost on a single curve at each T, indicating that thermodynamic properties of the two types of polymer in the *concentrated region* are determined substantially by the number of segments in the chains. We searched for an empirical equation for $J_{conc}(\bar{\phi})$, i.e., J applicable to the two polymers in the *concentrated region*. The resulting expression reads

$$J_{conc}(\bar{\phi}) = J_{c0} + J_{c1}\bar{\phi} + J_{c2}\bar{\phi}^2 \qquad (T \le \Theta) \qquad (8)$$

with

$$J_{c0} = 0.17(1 - \Theta/T) + 0.3(1 - \Theta/T)^2$$

$$J_{c1} = 0.11 + 1.5(1 - \Theta/T)$$

$$J_{c2} = 0.9 + 4.0(1 - \Theta/T) \qquad (9)$$

In the *dilute region*, J's for the star polymer tend to deviate upward from those for the linear polymer as the temperature decreases. This deviation comes primarily from the difference in J_0 (or A_2) between the two polymers, as may be seen from Figure 6, in which the values of J_0 for our star samples[13] are shown to be almost independent of molecular weight and larger than

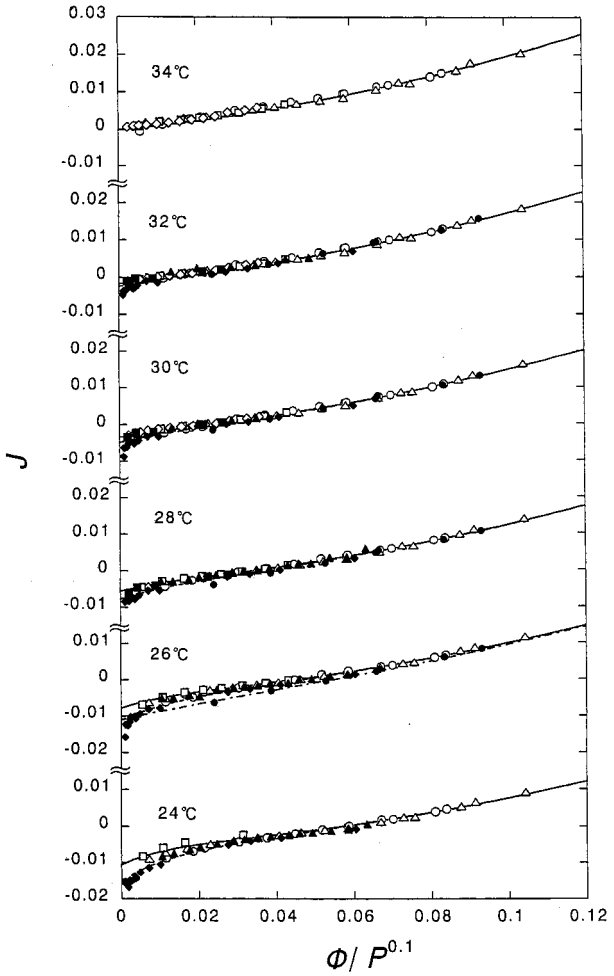

Figure 5. Plots of J vs $\phi/P^{0.1}$ for cyclohexane solutions of four-arm star [○, 4S22; △, 4S39; □, 4S77′; ◇, 4S384] and linear[8,9] [●, $M_w = 4.53 \times 10^4$; ◆, $M_w = 1.80 \times 10^5$; ▲, $M_w = 2.00 \times 10^5$; ■, $M_w = 4.98 \times 10^5$] polystyrenes in cyclohexane at the indicated temperatures. The solid and dashed lines represent the values calculated from eq 12 with eqs 8, 9, 10, 11, and 13 for sample 4S39 and linear polystyrene with $M_w = 1.80 \times 10^5$, respectively. The dotted−dashed line refers to linear polystyrene with the lowest molecular weight of 4.53×10^4 at 26 °C.

those (the dashed line) for the linear polymer represented empirically by[9]

$$J_0 = 0.26(1 - \Theta/T) - 4.6(1 - \Theta/T)^2 \qquad \text{(linear)} \quad (10)$$

The solid line fitting the data points for the star polymer

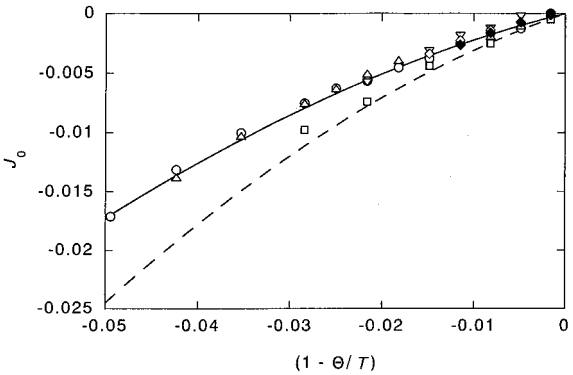

Figure 6. Plots of J_0 vs $(1 - \Theta/T)$ for four-arm star polystyrene in cyclohexane:[13] ○, 4S22; △, 4S39; □, 4S77′; ▽, $M_w = 8.05 \times 10^5$; ◊, 4S384; ♦, $M_w = 3.12 \times 10^6$. The solid and dashed lines represent the values calculated from eqs 11 and 10, respectively.

is expressed as

$$J_0 = 0.19(1 - \Theta/T) - 3.1(1 - \Theta/T)^2 \qquad \text{(star)} \quad (11)$$

With regard to A_2, two remarks are pertinent here.

1. In the molecular weight range studied in this work, A_2 for four-arm star polystyrene in cyclohexane was essentially zero at the Θ temperature (307.7 K).[13]

2. Yamakawa et al.[20] recently found that A_2 for linear polystyrene in cyclohexane below Θ is described by the double-contact approximation theory based on the random flight model. In this approximation, however, A_2 below Θ is lower for star polymers than for linear polymers,[21] contradicting the experimental data shown in Figure 6. Hence, A_2 below Θ (especially for four-arm star polymers) ought to be explored theoretically.

The above functions J_0 and $J_{conc}(\bar{\phi})$ may be interpolated with the aid of an exponential function[9,22] as

$$J = (J_0 - J_{c0}) \exp(-\phi/b) + J_{conc}(\bar{\phi}) \qquad (12)$$

We have set $b = (\text{constant})P^{-1/2}$ according to Einaga et al.[9] and determined the constant by curve fitting of the data points in Figure 5 as

$$b = [1.5 + 6.0(1 - \Theta/T)]/P^{1/2} \qquad \text{(linear)}$$

$$b = [0.9 + 2.0(1 - \Theta/T)]/P^{1/2} \qquad \text{(star)} \quad (13)$$

The solid and dashed curves in Figure 5 represent the J values calculated from eq 12 (with eqs 8−11 and 13) for sample 4S39 ($M_w = 1.55 \times 10^5$) and linear polystyrene samples with $M_w = 1.80 \times 10^5$, respectively. For clarity, the J values calculated for the other samples have been omitted, since the J vs $\bar{\phi}$ relations given by eq 12 are insensitive to P in the molecular weight range studied here; the dot−dash line, which refers to the lowest molecular weight sample of linear polystyrene ($M_w = 4.53 \times 10^4$) at 26 °C, deviates downward from the dashed line for the same T, but the deviation is small.

Phase Diagrams. We calculated the excess chemical potential $\mu_0 - \mu_0°$ as a function of ϕ, P, and T from eq 6 with eq 12 and also the excess chemical potential of the solute with the aid of the Gibbs−Duhem relation.[9] The binodals and spinodals computed for the four-arm star polymer samples with the resulting chemical potentials are shown by the solid and dashed lines, respectively, in Figure 3. They agree fairly well with the experimental data, indicating that the empirical J function consistently explains the present light-scattering and phase-separation data.

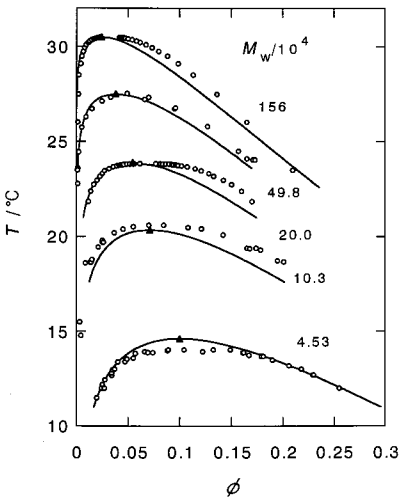

Figure 7. Binodals for cyclohexane solutions of linear polystyrene[16−18] with indicated M_w: unfilled circles, cloud points; solid lines, calculated binodals; filled triangles, calculated critical points (see text).

A similar comparison of the calculated and measured[8,9] binodals for the linear polymer is shown in Figure 7. The agreement is as good as that obtained by Einaga et al.,[9] who used a different expression for J. A point to note is that our J functions for the star and linear polymers with an identical P are the same in the *concentrated region*. In other words, the present analysis shows that the difference in $\mu_0 - \mu_0°$ between the two polymers and hence the effect of chain branching on phase equilibrium come entirely from that in $(J_0 - J_{c0}) \exp(-\phi/b)$.

The calculated critical temperatures for four-arm star and linear polystyrenes are also shown by solid and dashed lines, respectively, in Figure 4. These curves almost quantitatively explain the molecular weight dependence of T_c^{-1} for the two polymers, indicating that the difference in T_c between the two polymers arises from the apparent second virial coefficient in the *dilute region*.

Conclusions

The following conclusions may be derived from the present light-scattering and phase-separation studies on cyclohexane solutions of four-arm star polystyrene.

1. The apparent second virial coefficients J of light scattering for different degrees of polymerization plotted against $\phi/P^{0.1}$ at a fixed T below Θ form a composite curve at relatively high polymer concentrations. Literature J data for linear polystyrene samples in cyclohexane at comparable concentrations fall on the same curve.

2. On the other hand, in dilute solutions, J for four-arm star polystyrene is systematically larger than that for linear polystyrene, reflecting the difference in the second virial coefficient.

3. The chemical potentials of the solvent and solute components derived from J fairly satisfactorily explain the phase diagrams for the two polymer + solvent systems, and the lowering in the critical temperature by chain branching is due to the larger J for the star polymer in dilute solution. Examined in detail, however, the calculated binodals (Figures 3 and 7) and

spinodals (Figure 3) are seen not to fit precisely the data point. Near the critical points, the data points for each sample follow almost a flat curve, while the theoretical curve is convex upward with a significant curvature. This flat curve, common to both star and linear[9,16,23] polystyrenes, manifests the critical behavior discussed already by previous investigators.[16,23] It is clear that the chemical potential expression of the present form (or the *J* function) or that proposed by Einaga et al.[9] fails to describe this critical behavior. A more precise expression is needed for a more quantitative analysis of the phase behavior near the critical point.

References and Notes

(1) Kurata, M. *Thermodynamics of Polymer Solutions*; translated from the Japanese by H. Fujita; Harwood Academic Publishers: Chur, Switzerland, 1982.
(2) Fujita, H. *Polymer Solutions*; Elsevier: Amsterdam, 1990.
(3) Cowie, J. M. G.; Horta, A.; McEwen, I. J.; Prochazka, K. *Polym. Bull.* **1979**, *1*, 329.
(4) Sato, S.; Okada, M.; Nose, T. *Polym. Bull.* **1985**, *13*, 277.
(5) Yokoyama, H.; Takano, A.; Okada, M.; Nose, T. *Polymer* **1991**, *32*, 3218.
(6) Scholte, T. G. *Eur. Polym. J.* **1970**, *6*, 1063.
(7) Scholte, T. G. *J. Polym. Sci., Polym. Phys. Ed.* **1971**, *9*, 1553.
(8) Einaga, Y.; Ohashi, S.; Tong, Z.; Fujita, H. *Macromolecules* **1984**, *17*, 527.
(9) Einaga, Y.; Tong, Z.; Fujita, H. *Macromolecules* **1985**, *18*, 2258.
(10) Higo, Y.; Ueno, N.; Noda, I. *Polym. J.* **1983**, *15*, 367.
(11) Merkle, G.; Burchard, W.; Lutz, P.; Freed, K. F.; Gao, J. *Macromolecules* **1993**, *26*, 2736.
(12) Okumoto, M.; Nakamura, Y.; Norisuye, T.; Teramoto, A. *Macromolecules* **1998**, *31*, 1615.
(13) Okumoto, M.; Terao, K.; Nakamura, Y.; Norisuye, T.; Teramoto, A. *Macromolecules* **1997**, *30*, 7493.
(14) Deželić, Gj.; Vavra, J. *Croat. Chem. Acta* **1966**, *38*, 35.
(15) Rubingh, D. N.; Yu, H. *Macromolecules* **1976**, *9*, 681.
(16) Nakata, M.; Kuwahara, N.; Kaneko, M. *J. Chem. Phys.* **1975**, *62*, 4278.
(17) Hashizume, J.; Teramoto, A.; Fujita, H. *J. Polym. Sci., Polym. Phys. Ed.* **1981**, *19*, 1405.
(18) Tsuyumoto, M.; Einaga, Y.; Fujita, H. *Polym. J.* **1984**, *16*, 229.
(19) Noda, I.; Kato, N.; Kitano, T.; Nagasawa, M. *Macromolecules* **1981**, *14*, 668.
(20) Yamakawa, H.; Abe, F.; Einaga, Y. *Macromolecules* **1994**, *27*, 5704.
(21) Casassa E. F. *J. Chem. Phys.* **1962**, *37*, 2176.
(22) Koningsveld, R.; Stockmayer, W. H.; Kennedy, J. W.; Kleintjens, L. A. *Macromolecules* **1974**, *7*, 73.
(23) Kojima, J.; Kuwahara, N.; Kaneko, M. *J. Chem. Phys.* **1975**, *63*, 333.

MA980839N